Preprint typeset in JHEP style - PAPER VERSION

14 August 2006
FNT/T 2006/07
DFTT 14/2006
KA–TP–06–2006

Monte Carlo studies of the jet activity in Higgs + 2 jet events

Vittorio Del Duca

Istituto Nazionale di Fisica Nucleare, Sez. di Torino
via P. Giuria, 1 - 10125 Torino, Italy
E-mail: delduca@to.infn.it

Gunnar Klämke and Dieter Zeppenfeld

Institut für Theoretische Physik, Universität Karlsruhe
P.O. Box 6980, 76128 Karlsruhe, Germany
E-mail: klaemke@particle.uni-karlsruhe.de *and*
dieter@particle.uni-karlsruhe.de

Michelangelo L. Mangano

CERN, Theoretical Physics Division
CH 1211 Geneva 23, Switzerland
E-mail: michelangelo.mangano@cern.ch

Mauro Moretti

Dipartimento di Fisica, Università di Ferrara,
via Saragat, 1 - Ferrara, Italy
E-mail: mauro.moretti@fe.infn.it

Fulvio Piccinini

Istituto Nazionale di Fisica Nucleare, Sez. di Pavia
via A. Bassi, 6 - Pavia, Italy
E-mail: fulvio.piccinini@pv.infn.it

Roberto Pittau

Institute of Nuclear Physics, NCSR "Demokritos", 15-310 Athens, Greece
Dipartimento di Fisica Teorica Università di Torino and INFN Sez. di Torino
via P. Giuria, 1 - Torino, Italy
E-mail: pittau@to.infn.it

Antonio D. Polosa

Istituto Nazionale di Fisica Nucleare, Sez. di Roma
piazzale A. Moro, 2 - Roma, Italy
E-mail: polosa@roma1.infn.it

Abstract: Tree-level studies have shown in the past that kinematical correlations between the two jets in Higgs+2-jet events are direct probes of the Higgs couplings, e.g. of their CP nature. In this paper we explore the impact of higher-order corrections on the azimuthal angle correlation of the two leading jets and on the rapidity distribution of extra jets. Our study includes matrix-element and shower MC effects, for the two leading sources of Higgs plus two jet events at the CERN LHC, namely vector-boson and gluon fusion. We show that the discriminating features present in the previous leading-order matrix element studies survive.

Keywords: Standard Model, QCD, Higgs, Monte Carlo.

Contents

1. Introduction **1**

2. Numerical studies of Higgs + 2 jet events **2**

3. The azimuthal correlation **5**

4. The central–jet veto **7**

5. Conclusions **9**

1. Introduction

A major goal of the experiments at CERN's Large Hadron Collider (LHC) is the discovery of the Higgs boson and the study of its properties. Two processes dominate the production of a SM-like Higgs boson at the LHC, gluon fusion and vector-boson fusion (VBF). The latter is characterised by two forward tagging jets separated by a large rapidity interval, a feature that is very helpful to suppress backgrounds. However, also gluon fusion processes give rise to Higgs plus two jet production. For a measurement of Higgs couplings [1–3] it is important to distinguish these two sources of Hjj events [4]. In addition to the kinematical distributions of the two individual tagging jets, their correlations are markedly different for gluon fusion and vector boson fusion. For example, the dijet invariant mass distribution of the two leading jets in gluon fusion is substantially softer than in VBF.

A second characteristic difference emerges in the azimuthal correlations of the two tagging jets [5]. The distribution of the azimuthal angle $\Delta\phi_{jj}$ between the jets directly reflects the tensor structure of the coupling of the Higgs boson to weak bosons or gluons [6, 7]. The SM HWW and HZZ couplings, which arise from the kinetic energy term of the Higgs field, lead to a fairly flat $\Delta\phi_{jj}$ distribution. In contrast, the loop induced effective Hgg coupling, which, in the large top-mass limit, can be written as a CP-even effective Lagrangian proportional to $HG^a_{\mu\nu}G^{a,\mu\nu}$, produces a pronounced dip in the $\Delta\phi_{jj}$ distribution at 90 degrees, while a CP-odd coupling proportional to $HG^a_{\mu\nu}\tilde{G}^{a,\mu\nu}$ leads to striking minima at 0 and 180 degrees. Here $G^{a,\mu\nu}$ and $\tilde{G}^{a,\mu\nu} = \frac{1}{2}\varepsilon^{\mu\nu\rho\sigma}G^a_{\rho\sigma}$ denote the gluon field strength and its dual. The same correlation and similar dynamical properties were used in Refs. [6, 7] to discriminate between the Standard Model coupling and anomalous (New Physics) couplings between the Higgs and electroweak vector bosons.

The analyses of Refs. [5–7] were done at the parton level only. Previous experience with the azimuthal correlation between two jets at large rapidity intervals in dijet production in $p\bar{p}$ collisions, analysed at the parton level [8–12] and with parton showers and

hadronisation [13,14], and measured at the Tevatron [15], leads us to expect that a certain amount of de-correlation between the jets will be induced by showering and hadronisation, reducing the correlation induced by the dynamical properties of Higgs + 2 jet production at the parton level. Indeed, a much weaker correlation between the tagging jets in Higgs + 2 jet production via gluon fusion has been found after showering and hadronisation [16]. The analysis of Ref. [16] does not allow, though, for a direct comparison with the result of Ref. [5], because in Ref. [16] the two tagging jets associated to the Higgs production are generated by the parton shower and not by the matrix element. Thus, it is not possible to distinguish the decorrelation due to showering and hadronisation from an inherent lack of correlation between the two tagging jets caused by the approximations in the parton shower generation.

In the present work we address the shortcomings of either a purely hard matrix element calculation or of a purely parton-shower approach. We use ALPGEN [17, 18] to calculate the matrix elements for emission of hard partons and to then evolve the parton level events through the shower and hadronisation phases using HERWIG [14]. The effective ggH coupling is implemented in ALPGEN in the limit $m_t \to \infty$, where m_t is the top-quark mass. With this coupling, exact tree level matrix elements for $gg \to H$ plus additional hard partons are calculated. Subprocesses with initial- and final-state quarks are also included. As long as the Higgs mass and the parton transverse energies are smaller than the top-quark mass, the matrix elements can be evaluated with a very good approximation in the infinite top-quark mass limit. This holds true even when parton-parton invariant masses exceed the top-quark mass [5,19]. Details of our numerical simulation are discussed in Section 2. We then use this simulation for a study of decorrelation effects in Section 3.

A second characteristic property of VBF Higgs production is the reduced probability for the emission of extra jets between the tagging jets, which is caused by the t-channel color singlet exchange nature of VBF [20–22]. This feature can be exploited by a central jet veto for reducing QCD backgrounds to VBF, while at the same time reducing gluon fusion contamination to the VBF Higgs signal. In Section 4 we study the effects of the parton shower on the efficiency of the central jet veto. Conclusions are given in Section 5.

2. Numerical studies of Higgs + 2 jet events

For the numerical studies presented in this paper the Higgs mass is fixed to the value of 120 GeV, but the main results are independent of this choice. We generated unweighted event samples with ALPGEN for $H+2$ and $H+3$ hard partons (both for gluon fusion and for VBF processes), using two different partonic event selections,

$$a) \qquad p_{\mathrm{T}j}^{tag} > 30 \text{ GeV}\,, \qquad p_{\mathrm{T}j} > 20 \text{ GeV}\,, \qquad |\eta_j| < 5\,, \qquad R_{jj} > 0.6 \tag{2.1}$$

and

$$b) \qquad p_{\mathrm{T}j}^{tag} > 15 \text{ GeV}\,, \qquad p_{\mathrm{T}j} > 10 \text{ GeV}\,, \qquad |\eta_j| < 5\,, \qquad R_{jj} > 0.3\,, \tag{2.2}$$

where $p_{\mathrm{T}j}$ is the transverse momentum of a final-state parton and R_{jj} describes the separation of the two partons in the pseudo-rapidity, η, versus azimuthal angle plane,

$$R_{jj} = \sqrt{\Delta\eta_{jj}^2 + \Delta\phi_{jj}^2}\,. \tag{2.3}$$

In order to enhance VBF with respect to gluon fusion [5, 23], we select the two partons with the highest transverse energy as the tagging partons of our events, and require them to pass the additional kinematical constraints

$$|\eta_{j1} - \eta_{j2}| > 4.2\,, \qquad \eta_{j1}\cdot\eta_{j2} < 0\,, \qquad m_{jj} > 600\ \mathrm{GeV}\,, \tag{2.4}$$

for selection a) and

$$|\eta_{j1} - \eta_{j2}| > 3.2\,, \qquad \eta_{j1}\cdot\eta_{j2} < 0\,, \qquad m_{jj} > 500\ \mathrm{GeV}\,, \tag{2.5}$$

for selection b), i.e. the two tagging partons must be well separated in rapidity, they must reside in opposite detector hemispheres and they must possess a large parton-parton invariant mass. Selection a) uses the cuts which are imposed on the reconstructed jets after showering already at the parton level. Selection b) relaxes many of these cuts at the parton level in order to study effects of migration across cut boundaries. We will find that the shapes of most of the distributions considered below are insensitive to such migration effects.

The partonic events are then processed by HERWIG, which adds the shower evolution*. Final states now consist of a Higgs boson plus a number of jets originating from the original hard partons and from the shower. The jets are defined via a cone algorithm using the routine `GETJET` [24], which uses a simplified version of the UA1 jet algorithm, with parameters given by

$$p_{\mathrm{T}j} > 20\ \mathrm{GeV}\,, \qquad |\eta_j| < 5\,, \qquad R = 0.6\,, \tag{2.6}$$

where R is the jet cone radius. The jets are required to satisfy the kinematical cuts

$$p_{\mathrm{T}j}^{tag} > 30\ \mathrm{GeV}\,, \qquad p_{\mathrm{T}j} > 20\ \mathrm{GeV}\,, \qquad |\eta_j| < 5\,, \qquad R_{jj} > 0.6\,. \tag{2.7}$$

Here, the two tagging jets are defined as the two jets of highest p_T. They must satisfy the additional constraints on separation in true rapidity and on dijet mass

$$|y_{j1} - y_{j2}| > 4.2\,, \qquad y_{j1}\cdot y_{j2} < 0\,, \qquad m_{jj} > 600\ \mathrm{GeV}\,, \tag{2.8}$$

for both cases, a) and b), of partonic event selection.

The factorisation scale μ_{F} is set to the geometric mean of the jet transverse energies. In Refs. [5, 19] it was noted that with the cuts of Eqs. (2.1) and (2.4) the matrix elements

*The results presented include parton shower effects on top of the matrix elements but neglect hadronisation. The scale at which the parton shower is terminated is the HERWIG default of the order of 1 GeV. We have checked that hadronisation effects change our results at an insignificant level.

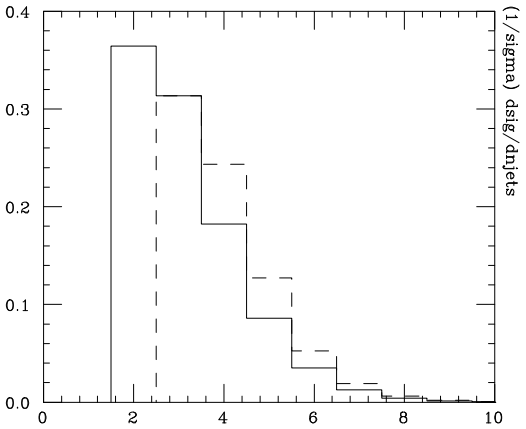

Figure 1: Normalised jet multiplicity after parton shower for the Higgs + 2 (solid) and 3 (dashes) final-state-parton production via gluon fusion.

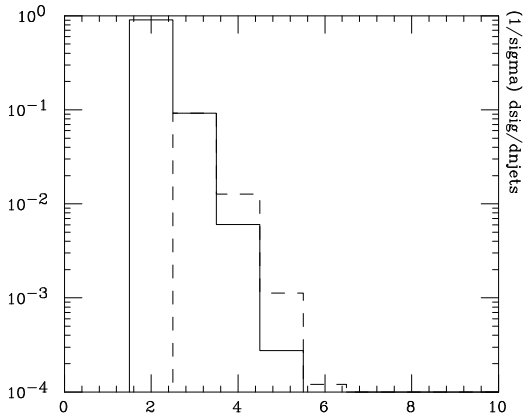

Figure 2: Normalised jet multiplicity as in the left panel, but with production via VBF. Note the log scale on the vertical axis.

for gluon fusion are dominated by gluon exchange in the t channel. Thus, as a scale for α_S, it is reasonable to choose, here and in what follows,

$$\alpha_S^4 \to \alpha_S^2(M_{\rm H})\alpha_S(p_{\rm T1})\alpha_S(p_{\rm T2}) \qquad \text{or} \qquad \alpha_S^5 \to \alpha_S^2(M_{\rm H})\alpha_S(p_{\rm T1})\alpha_S(p_{\rm T2})\alpha_S(p_{\rm T3}) \tag{2.9}$$

in the production of 2 or 3 jets in gluon fusion. For VBF the α_s renormalisation scale is taken equal to $\mu_{\rm F}$, i.e. the geometric mean of the jet transverse energies.

In Fig. 1 we show the jet-multiplicity distributions for gluon-fusion events, using the ALPGEN matrix elements for Higgs + 2 (solid) and 3 (dashes) final-state partons, evolved with the HERWIG parton shower. We use the partonic event selection a) of Eqs. (2.1) and (2.4). Reconstructed jets after the parton shower must satisfy the cuts of Eqs. (2.7) and (2.8). The solid curve is normalised to the total cross section for Higgs + 2-jet production (the bins add to one), while the dashed curve is normalised such that the 3-jet bin coincides with the 3-jet fraction of the $H + 2$ parton generated events[†]. Fig. 2 is the same as Fig. 1, but with VBF as the production mechanism. We note that in VBF the number of jets typically coincides with the number of generated final-state partons. In gluon fusion, however, a majority of the jets that pass the cuts of Eq. (2.7) arise from the parton shower, and in almost 70% of $H + 2$ parton generated events of selection a) this includes one of the tagging jet candidates, which then frequently fails the rapidity separation or dijet invariant mass cuts of Eq. (2.8). As a consequence we do not, here, calculate $H + 2$ jet total cross sections including parton shower effects.

A measure of the potential influence of this large shower activity on distributions is the extent to which the tagging jets after all cuts originate from the two leading $p_{\rm T}$ partons. We quantify this by determining the relative fraction of events where none, one or both tagging jets cointain within their cone the direction of a leading $p_{\rm T}$ parton. This distribution is shown in Figs. 3 and 4 for the partonic sample with selection of Eqs. (2.1) and (2.4), for

[†]The 2-jet bin of the $H + 3$ parton contribution is not shown since it has an unphysical dependence on the p_T cut of the third parton.

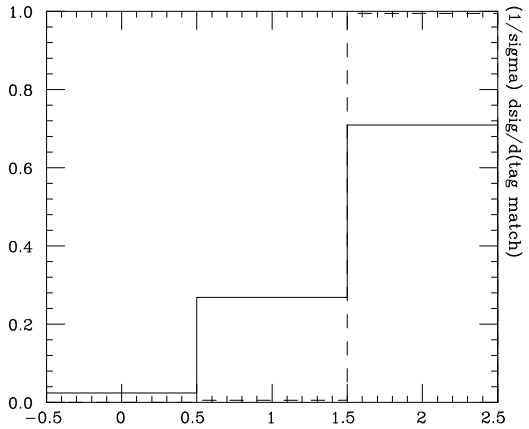

Figure 3: Fractions of events with 0, 1 and 2 tagging jets containing the original hard partons in Higgs + 2 parton generated production via gluon fusion (solid) and via VBF (dashes).

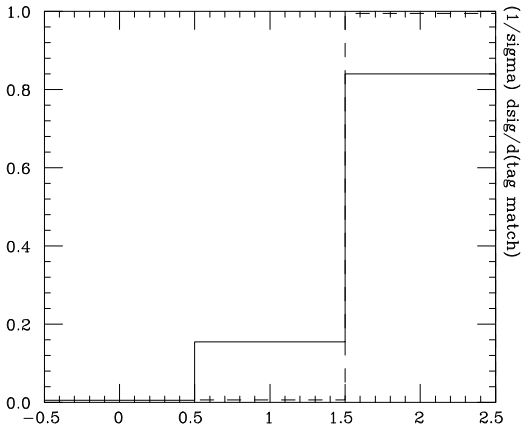

Figure 4: Same as Fig. 3, but for Higgs + 3 final-state-parton generated events.

2 and 3 final-state partons, respectively. The solid (dashed) curves correspond to gluon fusion (VBF). While for VBF there is a one-to-one correspondence between tagging jets and hard partons, both in Higgs + 2 partons and Higgs + 3 partons samples, in the case of production via gluon fusion there is a sizable sensitivity to the partonic cuts: for instance, for Higgs + 2 partons via gluon fusion the probability of having only one hard parton originating a tagging jet is at the level of 25% with the event selection *a*) of Eqs. (2.1) and (2.4). This probability grows to about 40% using the event selection *b*) of Eqs. (2.2) and (2.5). The probabilities are quite insensitive to variations of the $p_{\mathrm{T}j}^{tag}$ threshold in the range 30-50 GeV.

3. The azimuthal correlation

As discussed in the Introduction, the azimuthal distance between the two tagging jets, $\Delta\phi_{jj}$, is a sensitive measure of the structure of the Higgs coupling to gauge bosons. In Fig. 5, we evaluate this azimuthal correlation in Higgs + 2 jet production via gluon fusion with (solid) and without (dot–dashes) parton showers, and via VBF with parton showers (dashes), using the matrix elements for Higgs + 2 final-state partons[‡]. We note that the dip at $\Delta\phi_{jj} = \pi/2$ in Fig. 5 is somewhat shallower than in the parton-level results of Ref. [5] (solid histogram *vs.* dot–dashed curve) since, as expected, the additional radiation due to the showering dilutes the correlation between the jets. On the other hand, the dip is much deeper than in Ref. [16], where the tagging jets were generated by the soft radiation of the shower.

In addition, Fig. 5 confirms that, as found in Ref. [5], the tagging jets prefer to be back-to-back rather than collinear, leading to an asymmetry with respect to the dip at $\Delta\phi_{jj} = \pi/2$. Conversely, the distribution of Ref. [16] is symmetric.

[‡]The VBF plot without parton showers is not reported because it is identical to the one with showers.

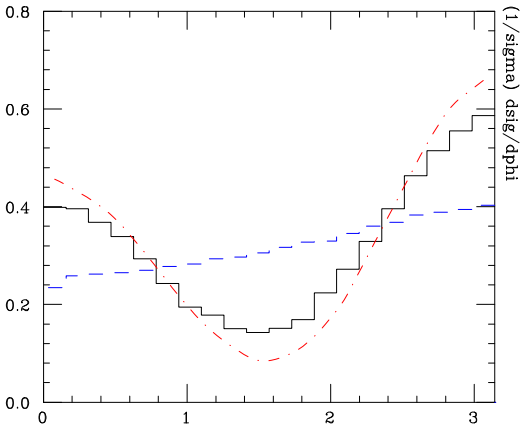

Figure 5: Normalised distribution of the azimuthal distance between the two tagging jets in Higgs + 2 parton production via gluon fusion, with (solid histogram) and without (dot–dashed curve) parton shower, and via VBF with parton shower (dashes).

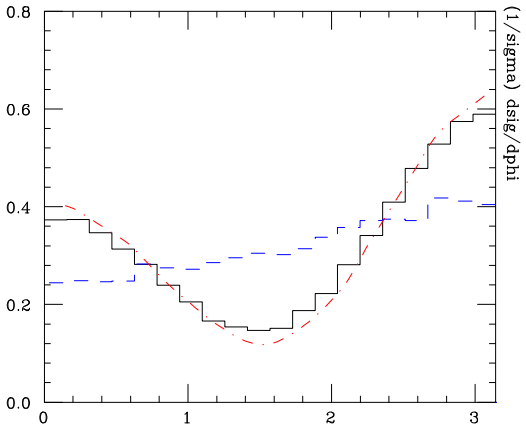

Figure 6: Normalised distribution of the azimuthal distance between the two tagging jets as in Fig. 5, but for Higgs + 3 parton production.

A_ϕ	parton level	shower level
$ggH + 2$ jets	0.474(3)	0.357(3)
$VBF + 2$ jets	0.017(1)	0.018(1)
$ggH + 3$ jets	0.394(4)	0.344(4)
$VBF + 3$ jets	0.022(3)	0.024(3)

Table 1: The quantity A_ϕ as defined in Eq. (3.1), for event selection a).

We conclude that although it is desirable to include showering and hadronisation for a quantitative analysis of the azimuthal correlation between two tagging jets in Higgs + 2 jet production, it is mandatory to generate the tagging jets through the hard radiation of the appropriate matrix elements. In Fig. 6 we consider the azimuthal correlation between the two tagging jets in Higgs + 3 parton generated production. The curves have the same meaning as in Fig. 5. It is apparent that the hard radiation of a third jet does not modify the pattern established in Fig. 5.

In order to characterise the $\Delta\phi_{jj}$ distribution and quantify the relative depth of the dip at $\Delta\phi_{jj} = \pi/2$, it is useful to introduce the following quantity,

$$A_\phi = \frac{\sigma(\Delta\phi < \pi/4) - \sigma(\pi/4 < \Delta\phi < 3\pi/4) + \sigma(\Delta\phi > 3\pi/4)}{\sigma(\Delta\phi < \pi/4) + \sigma(\pi/4 < \Delta\phi < 3\pi/4) + \sigma(\Delta\phi > 3\pi/4)}, \tag{3.1}$$

which is free of the normalisation uncertainties affecting the gluon-fusion production mechanism. A_ϕ can be used as a probe of the nature of the Higgs coupling, since for a SM gauge coupling $A_\phi \simeq 0$, while for a CP-even (CP-odd) effective coupling A_ϕ is positive (negative) [7]. As can be seen from Table 1, it is very close to zero for VBF, while it is positive for gluon fusion. Adding the parton shower on top of Higgs + 2 partons, the value of A_ϕ decreases, quantifying the effect of the decorrelation between the tagging jets introduced

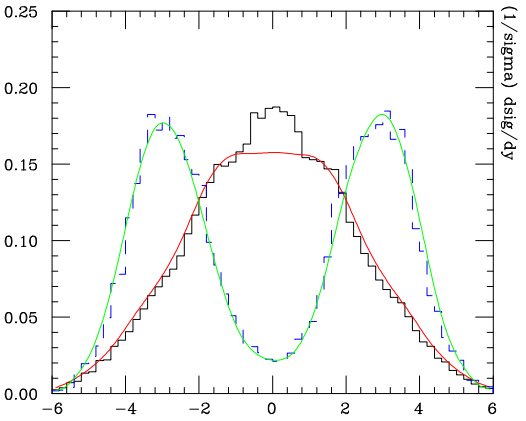

Figure 7: Normalised distribution of the rapidity of the third jet, measured with respect to the rapidity average of the two tagging jets in Higgs + 3 parton events after the parton shower, via gluon fusion (solid) and via VBF (dashed histogram). Also shown are the pure parton level expectations, generated with Higgs + 3 parton matrix elements, for gluon fusion (red curve) and VBF (green curve).

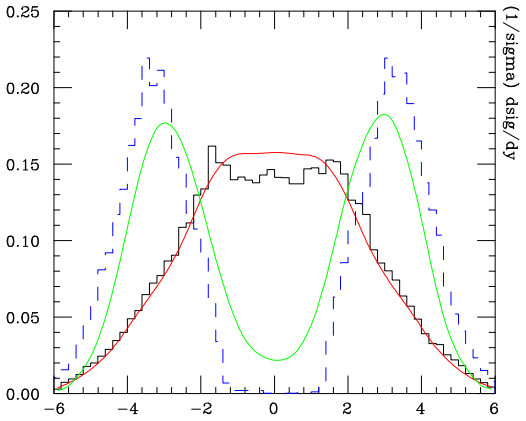

Figure 8: Normalised distribution of the rapidity of the third jet, as in Fig. 8, but for Higgs + 2 parton generated events after the shower.

by the shower. The decorrelation in $H + 2$ parton-generated gluon-fusion events reduces A_ϕ by about 25%. The generation of a third hard parton at the matrix element level already incorporates about 70% of this decorrelation effect. The numbers quoted in Table 1 refer to the partonic event selection *a*). However, they are quite insensitive to the partonic generation cuts: using the event selection *b*) reproduces the numbers of Table 1 within deviations of about 10%.

4. The central–jet veto

A distinguishing feature of Higgs production via VBF is that to leading order no colour is exchanged in the t-channel [20–22]. To $\mathcal{O}(\alpha_S)$, gluon radiation occurs only as bremsstrahlung off the quark legs: since no colour is exchanged in the t-channel in the Born process, no gluon exchange is possible to $\mathcal{O}(\alpha_S)$, except for a tiny contribution due to equal-flavour quark scattering with $t \leftrightarrow u$ channel exchange.

The different gluon radiation pattern expected for Higgs production via VBF compared to its major backgrounds, namely $t\bar{t}$ production and QCD $WW + 2$ jet production, is at the core of the central-jet veto proposal, both for heavy [25] and light [26] Higgs searches. A veto of any additional jet activity in the central rapidity region is expected to suppress the backgrounds more than the signal, because the QCD backgrounds are characterised by quark or gluon exchange in the t-channel. The exchanged partons, being coloured, are expected to radiate off more gluons.

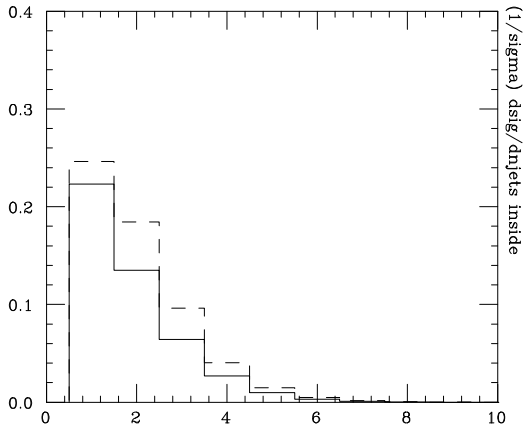

Figure 9: Normalised distribution of the multiplicity of the jets within the rapidity interval of the tagging jets, for the Higgs + 2 (solid) and 3 (dashes) final-state-parton production via gluon fusion.

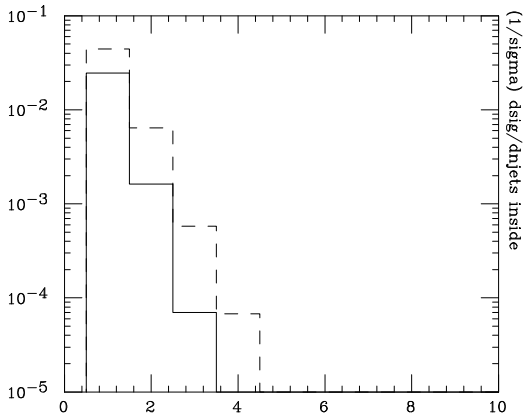

Figure 10: Normalised distribution of the multiplicity of the jets within the rapidity interval of the tagging jets, as in Fig. 9, but with production via VBF. Note the log scale on the vertical axis.

For the analysis of the Higgs coupling to gauge bosons, Higgs + 2 jet production via gluon fusion may also be treated as a background to VBF. When the two jets are separated by a large rapidity interval, the scattering process is dominated by gluon exchange in the t-channel. Therefore, like for the QCD backgrounds, the bremsstrahlung radiation is expected to occur everywhere in rapidity. An analogous difference in the gluon radiation pattern is expected in $Z + 2$ jet production via VBF fusion versus QCD production [27]. In order to analyse these features, in Ref. [28] the distribution in rapidity of a third jet was considered in Higgs + 3 jet production via VBF and via gluon fusion, using the cuts of Eqs. (2.1) and (2.4), with the $p_{\rm T}$ threshold for tagging jets at 20 GeV. The analysis was done at the parton level only. It showed that in VBF the third jet prefers to be emitted close to one of the tagging jets, while in gluon fusion it is emitted anywhere in the rapidity region between the tagging jets. Thus, at least as regards the hard radiation of a third jet, the analysis of Ref. [28] confirmed the general expectations about the bremsstrahlung patterns in Higgs production via VBF versus gluon fusion.

When including jets that are generated via the parton shower, we define the third jet as the jet with the third highest transverse momentum, jets 1 and 2 being the two tagging jets. In Fig. 7, we consider the normalised distribution of the rapidity of the third jet, measured with respect to the rapidity average of the tagging jets, $y_{\rm rel} = y_{j3} - (y_{j1} + y_{j2})/2$, in Higgs + 2 jet production via gluon fusion, with (black) and without (red) parton showers, and via VBF with (dashes) and without (green) parton showers for the additional radiation. We have used the matrix elements for Higgs + 3 final-state partons and the cuts of Eqs. (2.1) and (2.4). For VBF Fig. 7 confirms the parton-level results of [28], with the third jet more likely to be emitted in the vicinity of either of the tagging jets. For gluon fusion, on the other hand, we find that the third jet is emitted even more centrally in rapidity than predicted at the parton-level (black *vs.* red). In Fig. 8 we have repeated the analysis of Fig. 7, but we require the third jet to be generated by the soft radiation of the parton shower, *i.e.* we

have used the matrix elements for Higgs + 2 final-state partons, supplemented with the parton shower.

In order to quantify the jet activity in the rapidity interval between the tagging jets, we have computed the multiplicity distribution for jets that fall within this rapidity interval. The multiplicity is normalised with the same factors as in Figs. 1 and 2, *i.e.* to the total cross section for Higgs + 2-jet production after jet reconstruction. In Fig. 9 we show the distribution of the resulting additional jet multiplicity for Higgs + 2 (solid) and 3 (dashes) final-state-parton production via gluon fusion. Analogous results for VBF are shown in Fig. 10. In the multiplicity distribution of Fig. 10, note the large difference that arises between generating the third jet through the matrix element or through the parton shower. These deviations make the high-multiplicity values for the VBF process unreliable. Luckily, high jet multiplicities are very rare for VBF and, hence, this uncertainty is largely irrelevant phenomenologically.

5. Conclusions

In this work we have analysed some observables that distinguish the two main mechanisms for Higgs production, gluon fusion and vector-boson fusion, by looking at the jet activity and at the final-state event topology in Higgs + 2-jet events. In particular, we have considered the azimuthal correlation between the two tagging jets and a veto on the jet activity in the rapidity interval between the tagging jets. Our work builds upon previous parton-level work, by adding the parton-shower contribution. We have used ALPGEN to generate the appropriate matrix elements for the primary scattering, and have supplemented it with the parton showers generated by HERWIG.

In the case of the azimuthal correlation, we find that the dip at $\Delta\phi_{jj} = \pi/2$, characteristic of a CP-even Higgs boson produced via gluon fusion [5, 6], is slightly filled by the parton shower, but not as much as one would find by generating the tagging jets through the parton shower [16]. A measure of the dip filling is provided by the A_ϕ quantity (3.1). As regards the veto on the jet activity in the rapidity interval between the tagging jets, we have considered the rapidity distribution of the third jet, measured with respect to the rapidity average of the tagging jets. We confirm the parton-level findings of Ref. [28], namely that in gluon fusion the third jet is more likely to be emitted centrally in rapidity, while in VBF it is likely to be emitted in the vicinity of either of the tagging jets. In addition, to quantify the jet activity in the rapidity interval between the tagging jets, we have computed the multiplicity distribution of jets within the rapidity interval and normalised it to the total cross section for Higgs + 2-jet production, after jet reconstruction.

It must be stressed that leading-order calculations for multijet rates, as employed in this paper, may lead to an unphysical dependence of the jet cross sections on the parton-level generation cuts. For example, reducing to 0 the minimum $p_{\rm T}$ for the 3rd parton in the Higgs + 3-parton VBF channel will still allow the generation of events with 3 jets after the shower evolution, where the 3rd jet arises from radiation off the initial state or the two final-state hard partons. In absence of the appropriate virtual corrections or Sudakov suppression, the partonic cross section diverges when the $p_{\rm T}$ cut is sent to 0, and the rate

of these events can become unphysically large. In absence of a full NLO treatment, these issues can be addressed by a CKKW-like procedure [29–33], where such configurations are suppressed via the inclusion of the appropriate Sudakov form factors and the generation dependence is reduced. We plan to explore in more detail in a future study the implications of these issues for Higgs physics.

Acknowledgements

V. Del Duca, M. Moretti, F. Piccinini, R. Pittau and D. Zeppenfeld wish to thank the CERN Theory Division for its kind hospitality during the final stages of this work. The research of GK and DZ was supported by the Deutsche Forschungsgemeinschaft in the Sonderforschungsbereich/Transregio SFB/TR-9 "Computational Particle Physics" and in the Graduiertenkolleg "High Energy Physics and Particle Astrophysics". RP acknowledges the financial support of the ToK program "ALGOTOOLS" (MTKD-CT-2004-014319) and of MIUR (2004021808_009).

References

[1] D. Zeppenfeld, R. Kinnunen, A. Nikitenko and E. Richter-Was, *Measuring Higgs boson couplings at the LHC,* Phys. Rev. D **62** (2000) 013009 [hep-ph/0002036].

[2] A. Belyaev and L. Reina, *p p → t anti-t H, H → tau+ tau-: Toward a model independent determination of the Higgs boson couplings at the LHC,* JHEP **0208**, 041 (2002) [hep-ph/0205270].

[3] M. Duhrssen, S. Heinemeyer, H. Logan, D. Rainwater, G. Weiglein and D. Zeppenfeld, *Extracting Higgs boson couplings from LHC data,* Phys. Rev. D **70** (2004) 113009 [hep-ph/0406323].

[4] E. L. Berger and J. Campbell, *Higgs boson production in weak boson fusion at next-to-leading order,* Phys. Rev. D **70** (2004) 073011 [hep-ph/0403194].

[5] V. Del Duca, W. Kilgore, C. Oleari, C. Schmidt and D. Zeppenfeld, *Gluon-fusion contributions to H + 2 jet production,* Nucl. Phys. B **616** (2001) 367 [hep-ph/0108030].

[6] T. Plehn, D. L. Rainwater and D. Zeppenfeld, *Determining the structure of Higgs couplings at the LHC,* Phys. Rev. Lett. **88** (2002) 051801 [hep-ph/0105325].

[7] V. Hankele, G. Klamke and D. Zeppenfeld, *Higgs + 2 jets as a probe for CP properties,* hep-ph/0605117.

[8] V. Del Duca and C. R. Schmidt, *Dijet production at large rapidity intervals,* Phys. Rev. **D49** (1994) 4510 [hep-ph/9311290].

[9] W. J. Stirling, *Production of jet pairs at large relative rapidity in hadron-hadron collisions as a probe of the perturbative pomeron,* Nucl. Phys. **B423** (1994) 56 [hep-ph/9401266].

[10] V. Del Duca and C. R. Schmidt, *Azimuthal angle decorrelation in large rapidity Dijet production at the Tevatron,* Nucl. Phys. Proc. Suppl. **39BC** (1995) 137 [hep-ph/9408239].

[11] V. Del Duca and C. R. Schmidt, *BFKL versus O (alpha-s**3) corrections to large rapidity dijet production,* Phys. Rev. **D51** (1995) 2150 [hep-ph/9407359].

[12] L. H. Orr and W. J. Stirling, *Dijet production at hadron hadron colliders in the BFKL approach,* Phys. Rev. **D56** (1997) 5875 [hep-ph/9706529].

[13] G. Marchesini and B. R. Webber, *Monte Carlo Simulation Of General Hard Processes With Coherent QCD Radiation,* Nucl. Phys. **B310** (1988) 461.

[14] G. Marchesini, B. R. Webber, G. Abbiendi, I. G. Knowles, M. H. Seymour and L. Stanco, *HERWIG: A Monte Carlo event generator for simulating hadron emission reactions with interfering gluons. Version 5.1 - April 1991,* Comput. Phys. Commun. **67** (1992) 465.

[15] S. Abachi *et al.* [D0 Collaboration], *The Azimuthal decorrelation of jets widely separated in rapidity,* Phys. Rev. Lett. **77** (1996) 595 [hep-ex/9603010].

[16] K. Odagiri, *On azimuthal spin correlations in Higgs plus jet events at LHC,* JHEP **0303** (2003) 009 [hep-ph/0212215].

[17] M. L. Mangano, M. Moretti and R. Pittau, *Multijet matrix elements and shower evolution in hadronic collisions: W b anti-b + (n)jets as a case study,* Nucl. Phys. B **632** (2002) 343 [hep-ph/0108069].

[18] M. L. Mangano, M. Moretti, F. Piccinini, R. Pittau and A. D. Polosa, *ALPGEN, a generator for hard multiparton processes in hadronic collisions,* JHEP **0307** (2003) 001 [hep-ph/0206293].

[19] V. Del Duca, W. Kilgore, C. Oleari, C. R. Schmidt and D. Zeppenfeld, *Kinematical limits on Higgs boson production via gluon fusion in association with jets,* Phys. Rev. D **67** (2003) 073003 [hep-ph/0301013].

[20] Y. L. Dokshitzer, S. I. Troian and V. A. Khoze, *Collective QCD Effects In The Structure Of Final Multi - Hadron States. (In Russian),* Sov. J. Nucl. Phys. **46** (1987) 712 [Yad. Fiz. **46** (1987) 1220].

[21] Y. L. Dokshitzer, V. A. Khoze and T. Sjostrand, *Rapidity gaps in Higgs production,* Phys. Lett. B **274** (1992) 116.

[22] J. D. Bjorken, *Rapidity gaps and jets as a new physics signature in very high-energy hadron-hadron collisions,* Phys. Rev. **D47** (1993) 101.

[23] V. Del Duca, W. Kilgore, C. Oleari, C. Schmidt and D. Zeppenfeld, *H + 2 jets via gluon fusion,* Phys. Rev. Lett. **87** (2001) 122001 [hep-ph/0105129].

[24] F.E. Paige and S.D. Protopopescu, in *Physics of the SSC*, Snowmass, 1986, Colorado, edited by R. Donaldson and J. Marx.

[25] V. D. Barger, R. J. N. Phillips and D. Zeppenfeld, *Mini - jet veto: A Tool for the heavy Higgs search at the LHC,* Phys. Lett. B **346** (1995) 106 [hep-ph/9412276].

[26] N. Kauer, T. Plehn, D. Rainwater and D. Zeppenfeld, *$H \to W\,W$ as the discovery mode for a light Higgs boson,* Phys. Lett. B **503** (2001) 113 [hep-ph/0012351].

[27] D. Rainwater, R. Szalapski and D. Zeppenfeld, *Probing color-singlet exchange in Z + 2-jet events at the LHC,* Phys. Rev. D **54** (1996) 6680 [hep-ph/9605444].

[28] V. Del Duca, A. Frizzo and F. Maltoni, *Higgs boson production in association with three jets,* JHEP **0405** (2004) 064 [hep-ph/0404013].

[29] S. Catani, F. Krauss, R. Kuhn and B. R. Webber, *QCD matrix elements + parton showers,* JHEP **0111** (2001) 063 [hep-ph/0109231].

[30] L. Lonnblad, *Correcting the colour-dipole cascade model with fixed order matrix elements,* JHEP **0205** (2002) 046 [arXiv:hep-ph/0112284].

[31] M.L. Mangano, presentation at the 2nd meeting of the ME/MC tuning working group,FNAL, Nov 15 2002, http://cepa.fnal.gov/psm/MCTuning//15nov2002.html

[32] F. Krauss, *Matrix elements and parton showers in hadronic interactions,* JHEP **0208** (2002) 015 [hep-ph/0205283].

[33] S. Hoche, F. Krauss, N. Lavesson, L. Lonnblad, M. Mangano, A. Schalicke and S. Schumann, *Matching parton showers and matrix elements,* hep-ph/0602031.